axis changed orientation simultaneously, not by propagation, ~100 kyr ago. In addition to the gravitational collapse of orogenically overthickened lithosphere, causes for the opening of the Woodlark basin have been sought in the 'pull' of the Solomon Sea lithosphere which is being both subducted to the north at the New Britain trench and dragged northwestwards by the overriding Pacific plate[11,13]. Recent changes in the resultant of these additive forces, associated with spreading ridge and arc-continent collisions to the east and north respectively[38,39], may be responsible for the ridge reorientation. □

Received 3 November 1994; accepted 6 March 1995.

1. Falvey, D. A. *Aust. Petrol. Explor. Ass. J.* **14,** 95–106 (1974).
2. Karner, G. D., Driscoll, N. W. & Weissel, J. K. *Earth planet. Sci. Lett.* **114,** 397–416 (1993).
3. Klitgord, K. D. & Behrendt, J. C. in *Geological and Geophysical Investigations of Continental Margins* (eds Watkins, J. S., Montadert, L. & Dickerson, P. W.) 85–112 (Am. Ass. Petrol. Geologists, Tulsa, Oklahoma, 1979).
4. Lister, G. S., Etheridge, M. A. & Symonds, P. A. *Geology* **14,** 246–250 & 891–892 (1986).
5. Montadert, L., de Charpal, O., Roberts, D., Guennoc, P. & Sibuet, J.-C. in *Deep Drilling Results in the Atlantic Ocean: Continental Margins and Paleoenvironment* (eds Tlwani, M., Hay, W. & Ryan, W. B. F.) 154–186 (Am. Geophys. Un., Washington DC, 1979).
6. Tucholke, B. E., Austin, J. A. & Uchipi, E. in *Extensional Tectonics and Stratigraphy of the North Atlantic Margins* (eds Tankard, A. J. & Balkwill, H. R.) 247–263 (Am. Ass. Petrol. Geologists, Tulsa, Oklahoma, 1979).
7. Hey, R. N., Duennebier, F. K. & Morgan, W. J. *J. geophys. Res.* **85,** 2647–2658 (1980).
8. Courtillot, V. *Tectonics* **1,** 239–250 (1982).
9. Martin, A. K. *Tectonics* **3,** 611–617 (1984).
10. Cochran, J. R. & Martinez, F. *Tectonophysics* **153,** 25–53 (1988).
11. Weissel, J. K., Taylor, B. & Karner, G. D. *Tectonophysics* **87,** 253–277 (1982).
12. Taylor, B. in *Marine Geology, Geophysics and Geochemistry of the Woodlark Basin—Solomon Islands* (eds Taylor, B. & Exon, N. F.) 25–48 (Circum-Pacific Council for Energy & Mineral Resources, Houston, Texas, 1987).
13. Benes, V., Scott, S. D. & Binns, R. A. *J. geophys. Res.* **99,** 4439–4455 (1994).
14. Finlayson, D. M. *et al. Geophys. J. R. astr. Soc.* **29,** 245–253 (1976).
15. Smith, I. E. & Simpson, C. J. *Bull. Bur. Miner. Resour. Geol. Geophys. Aust.* **125,** 29–35 (1972).
16. Davies, H. L. *Am. J. Sci.* **280-A,** 171–191 (1980).
17. Davies, H. L. & Warren, R. G. *Tectonics* **7,** 1–21 (1988).
18. Davies, H. L. & Warren, R. G. *Contr. Miner. Petrol.* **112,** 463–474 (1992).
19. Hill, E. J., Baldwin, S. L. & Lister, G. S. *Geology* **20,** 907–910 (1992).
20. Hill, E. J. & Baldwin, S. L. *J. metamorph. Geol.* **11,** 261–277 (1993).
21. Baldwin, S. L., Lister, G. S., Hill, E. J., Foster, D. A. & McDougall, I. *Tectonics* **12,** 611–628 (1993).
22. Smith, I. E. M. & Milsom, J. S. in *Marginal Basin Geology* (eds Kokelar, B. P. & Howells, M. F.) 163–171 (Geol. Soc. Spec. publ. 16, Blackwell, Oxford, 1984).
23. Hegner, E. & Smith, I. E. M. *Chem. Geol.* **97,** 233–249 (1992).
24. Stolz, A. J., Davies, G. R., Crawford, A. J. & Smith, I. E. M. *Miner. Petrol.* **47,** 103–126 (1993).
25. Abers, G. A. *Geology* **19,** 1205–1208 (1991).
26. Taylor, B., Martinez, F., Hey, R. & Goodliffe, A. (abstr.) *Eos* **74,** 606 (1993).
27. Goodliffe, A., Taylor, B., Hey, R. & Martinez, F. (abstr.) *Eos* **74,** 606 (1993).
28. Binns, R. A. *et al. Proc. Pacif. Rim Congr.* **87,** 531–535 (1987).
29. Mutter, J. C., Mutter, C. Z., Abers, G. & Fang, J. (abstr.) *Eos* **74,** 412 (1993).
30. Taylor, B. & Hayes, D. E. in *The Tectonic and Geologic Evolution of Southast Asian Seas and Islands: Part 2* (Hayes, D. E.) 23–56 (Am. Geophys. Un., Washington DC, 1983).
31. Binns, R. A. & Whitford, D. J. *Proc. Pacif. Rim Congr.* **87,** 525–534 (1987).
32. White, R. S. *Eos* **74,** 58 (1993).
33. Mutter, J. C. *Nature* **364,** 393–394 (1993).
34. Bonatti, E. *Nature* **316,** 33–37 (1985).
35. Bosworth, W. *Geology* **14,** 890–891 (1986).
36. Martinez, F., Fryer, P., Baker, N. A. & Yamazaki, T. *J. geophys. Res.* (in the press).
37. Deep Ocean Resources Development Co. *South Pacific Seafloor Atlas* sheets 10–11 (Jap. int. Coop. Ag./Metal (Min. Ag. Jap./S. Pacif. appl. Geosci. Comm., Tokyo, 1995).
38. Crook, K. A. W. & Taylor, B. *Mar. geophys. Res.* **16,** 65–89 (1994).
39. Abbott, L. D., Silver, E. A. & Galewsky, J. *Tectonics* **13,** 1007–1034 (1994).

ACKNOWLEDGEMENTS. This research benefited greatly from the dedicated support of all on board the RV *Moana Wave* during cruise 9304, the services of the Hawaii Mapping Research Group, and the GMT software of P. Wessel and W. Smith. This work was supported by the US NSF.

A common neural code for frequency- and amplitude-modulated sounds

Kourosh Saberi* & Ervin R. Hafter†

* Center for Hearing Research, Department of Psychology, University of Florida, Gainesville, Florida 32611, USA
† Department of Psychology, University of California at Berkeley, Berkeley, California 94720, USA

MOST naturally occurring sounds are modulated in amplitude or frequency; important examples include animal vocalizations and species-specific communication signals in mammals, insects, reptiles, birds and amphibians[1–9]. Deciphering the information from amplitude-modulated (AM) sounds is a well-understood process, requiring a phase locking of primary auditory afferents to the modulation envelopes[10–12]. The mechanism for decoding frequency modulation (FM) is not as clear because the FM envelope is flat (Fig. 1). One biological solution is to monitor amplitude fluctuations in frequency-tuned cochlear filters as the instantaneous frequency of the FM sweeps through the passband of these filters. This view postulates an FM-to-AM transduction whereby a change in frequency is transmitted as a change in amplitude[13,14]. This is an appealing idea because, if such transduction occurs early in the auditory pathway, it provides a neurally economical solution to how the auditory system encodes these important sounds. Here we illustrate that an FM and AM sound must be transformed into a common neural code in the brain stem. Observers can accurately determine if the phase of an FM presented to one ear is leading or lagging, by only a fraction of a millisecond, the phase of an AM presented to the other ear. A single intracranial image is perceived, the spatial position of which is a function of this phase difference.

In experiment 1 (Fig. 1) we led an FM sound to one ear and an AM to the other ear. Both sounds had the same sinusoidal modulation rate and carrier frequency. We imposed an interaural phase difference on the periodicities of modulation. The observer's task was to detect this phase disparity in a two-alternative, forced-choice task. Near-perfect discrimination is achieved when the FM is delayed by 2 ms, that is, half the modulation cycle. Performance is at chance (0.5 probability) when the FM is advanced by 4 ms, a full cycle of modulation. Observers report the percept of a single, intracranial image which is laterally displaced toward one ear. As the interaural phase difference exceeds 2 ms (π radians), the image's spatial position reverses towards the other ear, consistent with the iterative nature of periodic signals.

In experiment 2 we considered the properties of the envelope after transduction. For each cycle of modulation, the FM will pass twice through the central passband of a filter centred near the FM carrier: once for each direction of frequency sweep. The resultant AM will therefore have an envelope rate that is twice the FM rate. However, filters which are centred away from the FM carrier will produce AM at the same rate as the FM. For example, the FM may only sweep through the lower skirt of a filter centred above the carrier. There are many such filters both above and below the carrier frequency, and we therefore refer to this scheme as a global model. If the auditory system relies primarily on local information from filters centred near the carrier then it may miscode the modulation information. Figure 2 shows performance as a function of the FM carrier frequency and modulation rate with the AM carrier and rate fixed at 3 kHz and 250 Hz, respectively. The yellow pyramid shows equivalent FM and AM parameters. The red pyramids show equal rates but different carriers. Dark blue shows an FM rate equal to half the AM rate; good performance for dark blue supports a local model, whereas good performance for red and yellow suggests an avoidance of such misinformation in favour of using global information. Perhaps more striking is that interaural-delay sensitivity is maintained across very different carriers (red pyramids), further supporting a global model.

In experiment 3 an illusion of motion was successfully induced by linearly changing (sweeping) high-frequency tones at different rates in the two ears. Unidirectional spectral sweeps are abund-

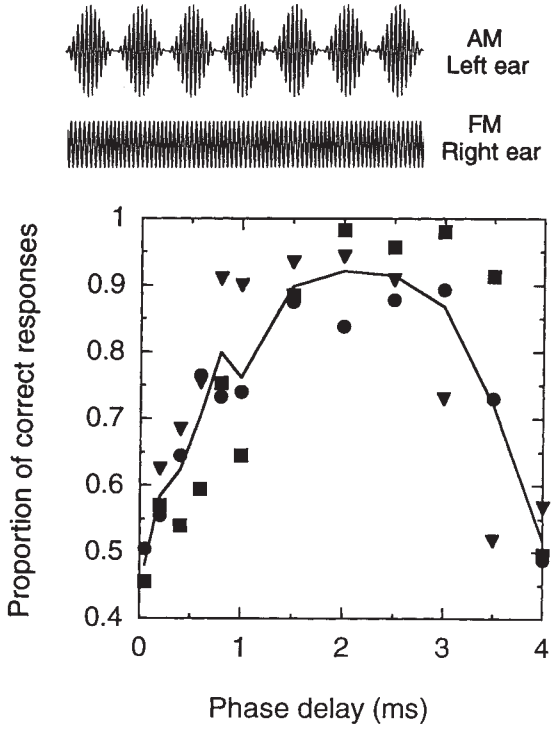

FIG. 1 Stimuli and results of experiment 1. The left ear received the AM signal and the right ear the FM. Ordinate shows proportion of correct detection of an interaural delay in a two-alternative, forced-choice task. Peak performance is observed when the 250-Hz sinusoidal modulators are antiphasic at the two ears (2 ms). Chance performance is 0.5. Different symbols represent different observers.
METHODS. Both FM and AM signals had a carrier of 3 kHz and a sinusoidal modulation rate of 250 Hz. Signals were 300 ms in duration with 20-ms cosine-squared ramps; the ramps were not interaurally delayed. Signals were digitally generated and presented at a sampling rate of 100 kHz and a level of 60 dB (2×10^{-5} N m^{-2}) through digital-to-analog converters and Sennheiser (HD-450) headphones in a soundproof chamber. The AM had a 100% depth of modulation and the FM index of modulation was unity. Experimental controls included intense low-pass noise (1.5 kHz cutoff; $N_0 = 30$ dB); highpass filtering (1.5 kHz); or using signals with very low sound-pressure levels (30 dB). The Sennheiser headphone transfer function was flat within 0.8 dB from 2750 to 3250 Hz. Digital inverse filtering was used to eliminate this small variation in level.

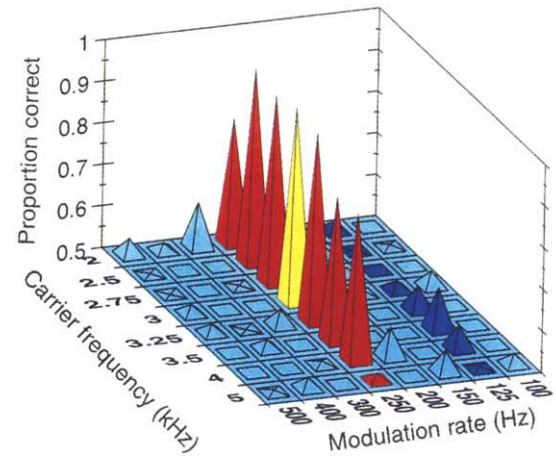

FIG. 2 Results of experiment 2. These data show interaural-delay sensitivity for unequal carriers and modulation rates. The left ear received a sinusoidal AM with a carrier of 3 kHz and a modulation rate of 250 Hz. The right ear received a sinusoidal FM, the carrier and modulation rate of which were parameters (x and y coordinates). Data were collected for all 64 combinations averaged across three observers. The yellow pyramid shows data for equivalent FM and AM rates and carriers. Red shows equivalent modulation rates but different carriers. Dark blue shows an FM rate half that of AM (see text). Methods were the same as Fig. 1.

ant naturalistic stimuli; the sonar emissions of the FM bat[1] and primate warning cells[15] are two examples. Recent behavioural[16] and physiological[17] observations provide evidence of a monaural code for directional sweeps, but not a binaural code. It has also been known for over a century[18,19] that binaural temporal cues are uninformative in high-frequency pure (unmodulated) tones. Tones, however, are unnatural stimuli and we reasoned that, even at high frequencies, a more natural sound created by spectrally sweeping the tone may generate impulsive rise-and-decay activity in successive, tonotopically ordered cochlear filters. A more rapid sweep in one ear would produce, relative to the other ear, correspondingly earlier neural activity in units tuned to similar frequency regions. In fact, observers reported a very strong illusion of intracranial spatial motion towards the ear that carried the faster sweep. In support of this subjective report, Fig. 3 shows binaural sensitivity to very small delays, in the order of only tens of microseconds.

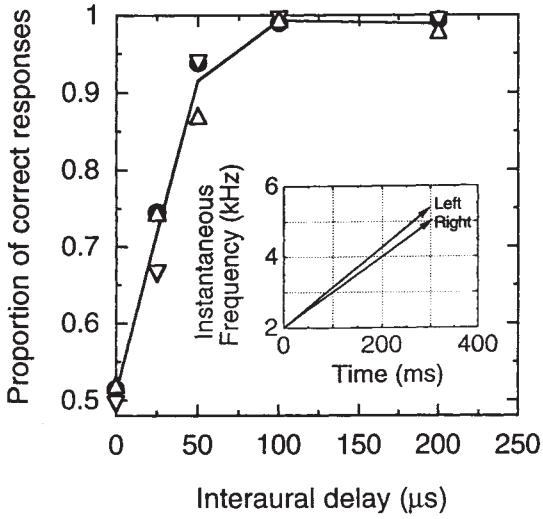

FIG. 3 Results of experiment 3. The inset shows stimuli used to induce the illusion of motion by spectrally sweeping tones in the two ears at different rates. The moving auditory image had a trajectory towards the ear which carried the faster sweep. Because motion is a subjective phenomenon, to validate these results psychophysically, the data in the figure were collected for the special case where the sweeps at the two ears had the same spectral velocity (equal time–frequency slopes). This produced a spatially stationary image. The subject's task was to detect an interaural delay in the sweep in a two-alternative, forced-choice task. Chance performance is 0.5. The solid line shows mean performance. Each symbol represents data from one observer.
METHODS. The signal was a tone of 300 ms which spectrally swept from 2 to 5 kHz. The entire waveform, except for the gating envelopes, was delayed to one ear. To obscure pitch cues, the starting frequency (y-intercept) and the slope of the frequency sweep were independently randomized on each observation by 10%. The interaural frequency difference at 2 kHz produced by delaying the sweep by 50 μs is 1.5 Hz. Control tests showed that this cue was uninformative. The spectrum of the signal was symmetric about the sweep's terminal frequency. The amplitude of the 2–5 kHz sweep was down by 60 dB at 1.5 kHz.

The coding of information in modulated form extends to other sensory domains, for example, vision. Psychophysical experiments have illustrated visual sensitivity to AM and FM spatial frequencies[20-22]. Physiological studies have also identified units in areas 17 and 18 of the Cat visual cortex which respond to envelope information at high spatial frequencies[23]. Our results suggest that the auditory system uses a common neural code for both FM and AM information at relatively early neural stages, possibly before binaural convergence at the brain stem[24-26]. Units responsive to monaural frequency sweeps have previously been identified; some entrain to very high rates in the range in which we have reported excellent binaural sensitivity[17,27,28]. Although the binaural properties of such neurons have not been examined at any level of the auditory pathway, the results reported here encourage such a search. □

Received 19 December 1994; accepted 6 February 1995.

1. Simmons, J. A. *Science* **203,** 16–21 (1979).
2. Bailey, W. J., Greenfield, M. D. & Shelly, T. E. *J. Insect Behav.* **6,** 141–154 (1993).
3. Dear, P. S., Simmons, J. A. & Fritz, J. *Nature* **364,** 620–623 (1993).
4. Coscia, E. M., Phillips, P. D. & Fentress, J. C. *Bioacoustics* **3,** 275–293 (1991).
5. Robisson, P., Aubin, T. & Bremond, J. *Ethology* **94,** 279–290 (1993).
6. Huber, F. & Thorson, J. *Scient. Am.* **253** (6), 60–68 (1985).
7. Ryan, M. J. & Wilczynski, W. *Science* **240,** 1786–1788 (1988).
8. Klump, G. M. & Langemann, U. *Adv. Bioacoust.* **83,** 353–359 (1992).
9. Brillet, C. & Paillette, M. *Bioacoustics* **3,** 33–44 (1991).
10. Smith, R. & Brachman, M. *Hearing Res.* **2,** 123–133 (1980).
11. Javel, E. *J. acoust. Soc. Am.* **68,** 133–146 (1980).
12. Schreiner, C. E. & Langner, G. in *Auditory Function* (eds Edelman, G. M., Gall, W. E. & Cowan, W. M.) 337–361 (Wiley, New York, 1988).
13. Zwicker, E. *Acustica* **2,** 125–133 (1952).
14. Henning, G. B. *J. acoust. Soc. Am.* **68,** 446–454 (1980).
15. Masataka, N. *Primates* **24,** 40–51 (1983).
16. Shu, Z. J., Swindale, N. V. & Cynader, M. S. *Nature* **364,** 721–723 (1993).
17. Mendelson, J. R. & Cynader, M. S. *Brain Res.* **327,** 331–335 (1985).
18. Lord Rayleigh (J. W. Strutt) *Nature* **14,** 32–33 (1876).
19. Lord Rayleigh (J. W. Strutt) *Phil. Mag.* (Ser. 6) **13,** 214–220 (1907).
20. Henning, G. B., Hertz, B. G. & Broadbent, D. E. *Vision Res.* **15,** 887–898 (1975).
21. Carlson, C. R., Anderson, C. H. & Moeller, J. R. *Invest. Ophthalmol. Vis. Sci.* (suppl.), 165–166 (1980).
22. Jamar, J. H. T., Kwakman, F. T. & Koenderink, J. J. *Vision Res.* **24,** 243–249 (1984).
23. Zhou, Y. & Baker, C. L. Jr *Science* **261,** 98–101 (1993).
24. Kuwada, S., Yin, T. C. T. & Wickesberg, R. E. *Science* **206,** 586–588 (1979).
25. Yin, T. C. T. & Chan, C. K. *J. Neurophysiol.* **64,** 465–487 (1990).
26. Carr, C. E. & Konishi, M. *J. Neurosci.* **10,** 3227–3246 (1990).
27. Whitfield, I. C. & Evans, E. F. *J. Neurophysiol.* **28,** 655–672 (1965).
28. Rees, A. & Moller, A. R. *Hearing Res.* **10,** 301–330 (1983).

ACKNOWLEDGEMENTS. This work was supported by NIH (National Institute of Deafness and other Communicative Disorders). We thank D. M. Green, G. B. Henning, D. McFadden, R. L. DeValois, B. C. J. Moore, B. W. Edwards, E. A. Strickland and J. C. Middlebrooks for discussion.

Lifetime of the P-selectin–carbohydrate bond and its response to tensile force in hydrodynamic flow

Ronen Alon, Daniel A. Hammer* & Timothy A. Springer†

The Center for Blood Research and Department of Pathology, Harvard Medical School, Boston, Massachusetts 02115, USA
* School of Chemical Engineering, Cornell University, Ithaca, New York 14853, USA

SELECTINS tether to the blood vessel wall leukocytes that are flowing in the bloodstream and support subsequent labile rolling interactions as the leukocytes are subjected to hydrodynamic drag forces[1,2]. To support this rolling, selectins have been proposed to have rapid bond association and dissociation rate constants, and special mechanical properties linking tensile forces and bond dissociation[3-6]. We have visualized transient tethering and release of neutrophils in hydrodynamic flow on lipid bilayers containing densities of P-selectin below those required to support rolling. We report here that transient tethers had first-order kinetics and other characteristics suggesting a unimolecular interaction between P-selectin and its glycoprotein ligand (PSGL-1). The unstressed dissociation constant (off rate) was 1 s^{-1}. Hydrodynamic shear stresses of up to 1.1 dyn cm^{-2}, corresponding to a force on the bond of up to 110 pN, increased the off rate only modestly, to 3.5 s^{-1}. The data was adequately matched by a proposed equation[7] relating off rate to the exponential of tensile force on the bond and the bond interaction distance, and gave a bond interaction distance of 0.5Å. This distance is compatible with hydrogen and metal coordination bonds between P-selectin and PSGL-1. Fast on and off rates, together with the high tensile strength of the selectin bond, appear necessary to support rolling at physiological shear stresses.

We used video microscopy to visualize neutrophil adhesion in shear flow to P-selectin reconstituted in lipid bilayers in a parallel-wall flow chamber. At densities from 400 to 30 sites per μm^2 of P-selectin, neutrophils in hydrodynamic flow tethered to the bilayer and then rolled across it with a jerky motion. During rolling, cells paused for short periods of time, then translated forward for a distance of less than one cell diameter, perhaps reflecting dissociation of one and retention of other selectin–carbohydrate bonds (cell 3, Fig. 1*a*, *b*). At 15 or fewer P-selectin sites per μm^2, the jerkiness increased and periods during which the cells tethered or rolled were separated by periods during which the cell moved forward at the hydrodynamic velocity, the velocity predicted for a non-adherent cell in flow near the wall (Fig. 1*a*, cells 1 and 2)[8,9]. Tethering events were defined as transient when they were separated by at least 50 μm of motion at the hydrodynamic velocity, and when no rolling (<1 μm displacement) occurred while the cell was tethered. At 15 sites per μm^2, 67% of the tethering events were transient, and at 6, 5, 3 and 1 sites per μm^2, all tethering events were transient. The frequency of transient tethering was linearly related to P-selectin site density (Fig. 2). Tethering was highly specific because it was inhibited by pretreatment of the bilayers by monoclonal antibody to P-selectin, pretreatment of neutrophils with *O*-glycoprotease, or addition of EDTA (Fig. 2). This agrees with findings that the ligand for P-selectin on human neutrophils is a sialyl $Lewis^x$-like structure that is displayed by the mucin-like P-selectin glycoprotein ligand (PSGL-1), which is *O*-glycoprotease-sensitive, and that ligand binding requires Ca^{2+} (refs 10–12).

To determine the kinetics for release of tethered neutrophils from P-selectin bilayers (the cellular off rate) the duration of tethering events at a wall shear stress of 0.36 dyn cm^{-2} was measured for P-selectin densities from 1 to 30 sites per μm^2 (Fig. 3*a*). Each set of data from 1 to 15 sites per μm^2 fit a single straight line, demonstrating first-order kinetics. Furthermore, the cellular dissociation rate constant k_{off} was unaffected by P-selectin density from 1 to 15 sites per μm^2 (Fig. 3*a*, *b*). Although there may be heterogeneity in the structure of carbohydrate ligands for P-selectin displayed on PSGL-1[12], our finding of a single dissociation rate constant suggests the ligands are homogenous at least with respect to dissociation rate, and agrees with homogenous affinity[13].

The independence of cellular dissociation rate on P-selectin density at 15 sites per μm^2 and below, the lack of rolling, and the linear rather than higher-order dependence of tethering frequency on selectin density, suggest that a quantal tethering unit has been identified. The data are consistent with the hypothesis that this quantal tethering unit is a monovalent bond between a single PSGL-1 molecule on the neutrophil and a single P-

† To whom correspondence should be addressed.